ASTRONOMY

Oxygen isotopic heterogeneity in the early Solar System inherited from the protosolar molecular cloud

Alexander N. Krot[1,2]*, Kazuhide Nagashima[1], James R. Lyons[3], Jeong-Eun Lee[4], Martin Bizzarro[2]

The Sun is ^{16}O-enriched ($\Delta^{17}O = -28.4 \pm 3.6$‰) relative to the terrestrial planets, asteroids, and chondrules ($-7‰ < \Delta^{17}O < 3‰$). Ca,Al-rich inclusions (CAIs), the oldest Solar System solids, approach the Sun's Δ^{17}O. Ultraviolet CO self-shielding resulting in formation of ^{16}O-rich CO and ^{17,18}O-enriched water is the currently favored mechanism invoked to explain the observed range of Δ^{17}O. However, the location of CO self-shielding (molecular cloud or protoplanetary disk) remains unknown. Here we show that CAIs with predominantly low $(^{26}Al/^{27}Al)_0$, $<5 \times 10^{-6}$, exhibit a large inter-CAI range of Δ^{17}O, from −40‰ to −5‰. In contrast, CAIs with the canonical $(^{26}Al/^{27}Al)_0$ of $\sim 5 \times 10^{-5}$ from unmetamorphosed carbonaceous chondrites have a limited range of Δ^{17}O, −24 ± 2‰. Because CAIs with low $(^{26}Al/^{27}Al)_0$ are thought to have predated the canonical CAIs and formed within first 10,000–20,000 years of the Solar System evolution, these observations suggest oxygen isotopic heterogeneity in the early solar system was inherited from the protosolar molecular cloud.

INTRODUCTION

The oxygen isotopic composition of the Sun inferred from the measurements of the solar wind returned by the NASA Genesis spacecraft is ^{16}O-enriched [$\Delta^{17}O = -28.4 \pm 3.6$ per mil (‰)] relative to the whole-rock oxygen isotopic compositions of Mars, Moon, chondrites and achondrites, and oxygen isotopic compositions of chondrule phenocrysts, which, on a three-isotope oxygen diagram (δ^{17}O versus δ^{18}O), plot close to the terrestrial fractionation line ($-7‰ < \Delta^{17}O < 3‰$) (*1*–*6*). A unique nonporphyritic chondrule from the CH carbonaceous chondrite Acfer 214 is ^{16}O-enriched ($\Delta^{17}O \sim -36‰$) compared to the Sun (*7*). Most Ca,Al-rich inclusions (CAIs) and amoeboid olivine aggregates (AOAs) in unmetamorphosed, petrologic type 2 to 3.0, carbonaceous chondrites [CR2, CO3.0, Acfer 094 (C3.0 ungrouped), and spinel-hibonite inclusions (SHIBs) in CM2s] have uniform solar-like oxygen isotopic compositions with Δ^{17}O of −24 ± 2‰ (Fig. 1A) (*8*–*11*). In contrast, texturally fine-grained refractory inclusions in metamorphosed CO and CV chondrites of petrologic type >3.0 are isotopically heterogeneous with Δ^{17}O ranging from ~−30 to ~0‰ (*12*, *13*), most likely reflecting postcrystallization oxygen-isotope exchange with an external ^{16}O-poor reservoir (*6*). Although the observed range in Δ^{17}O of solids formed in the Solar System is commonly attributed to a mixing between the ^{16}O-rich and ^{16}O-poor reservoirs (*1*), the nature of these reservoirs and the timing of their generation in the protoplanetary disk are still poorly understood. An improved understanding of the timing of the processes would provide strong constraints on theories of Solar System formation.

It has been suggested that ultraviolet CO self-shielding could have resulted in the formation of ^{16}O-rich CO and ^{17,18}O-enriched H_2O with compositions that on a three-isotope oxygen diagram follow a ~slope-1 line (*14*–*17*). Subsequent dust/gas fractionation followed by high-temperature thermal processing in the protoplanetary disk is the currently favored mechanism invoked to explain the observed range of Δ^{17}O among extraterrestrial materials (*14*–*17*). The timing and location of the CO self-shielding remain unknown. Originally, it was hypothesized that this process occurred in the hot nebular region near the young Sun (*15*). However, under these conditions, the self-shielding effects in CO would have been rapidly erased by oxygen-isotope exchange (*18*). Subsequently, it was suggested that CO self-shielding took place either in the protosolar molecular cloud (*16*) or in the cold outer region of the protoplanetary disk, outside 30 astronomical units (AU) from the Sun, irradiated by a neighboring massive O or B star (*17*). The existence of an extremely ^{16}O-poor reservoir ($\Delta^{17}O \sim +80‰$) in the protoplanetary disk is supported by the discovery of an anomalously ^{16}O-depleted magnetite (Fe_3O_4) in the Acfer 094 cosmic symplectites that most likely formed by oxidation of Fe,Ni-metal by nebular water (*19*). However, the chronology of this process is not known.

Refractory inclusions are the oldest solids formed in the Solar System. The U-corrected Pb-Pb absolute ages of four CAIs from CV carbonaceous chondrites, 4567.3 ± 0.16 million years (Ma), define a cosmochemical time 0 (t_0) of the Solar System evolution (*20*). Refractory inclusions formed by evaporation, condensation, aggregation, and occasionally melting processes in a gas of approximately solar composition, in a hot protoplanetary disk region exposed to irradiation by solar energetic particles, most likely near the protosun (*6*, *21*, *22*). The presence of the mineralogically and isotopically distinct populations of CAIs in different carbonaceous chondrite groups (*22*–*24*) suggests that refractory inclusions formed episodically, potentially providing snapshots of isotopic evolution of the protoplanetary disk.

Refractory inclusions recorded heterogeneous distribution of ^{26}Al, a short-lived radionuclide that decays to ^{26}Mg with a half-life of ~0.7 Ma, in the early Solar System (*8*, *25*–*28*). ^{26}Al is thought to have been injected by a stellar wind from a nearby Wolf-Rayet star (*29*, *30*) or another massive star (*31*) into the initially ^{26}Al-poor protosolar molecular cloud shortly before or contemporaneously with its collapse. Most CAIs and AOAs in unmetamorphosed carbonaceous chondrites are characterized by the inferred initial $^{26}Al/^{27}Al$ ratio [$(^{26}Al/^{27}Al)_0$] of $\sim 5 \times 10^{-5}$, named the canonical ratio (*8*–*10*, *22*, *32*, *33*), hereafter referred to as ^{26}Al-rich CAIs. However, some refractory inclusions in the same meteorites [e.g., platy hibonite crystals (PLACs),

[1]Hawai'i Institute of Geophysics and Planetology, University of Hawai'i at Mānoa, Honolulu, HI, USA. [2]Centre for Star and Planet Formation, Globe Institute, University of Copenhagen, Denmark. [3]School of Earth and Space Exploration, Arizona State University, Tempe, AZ, USA. [4]Department of Astronomy and Space Science, School of Space Research, Kyung Hee University, Korea.
*Corresponding author. Email: sasha@higp.hawaii.edu

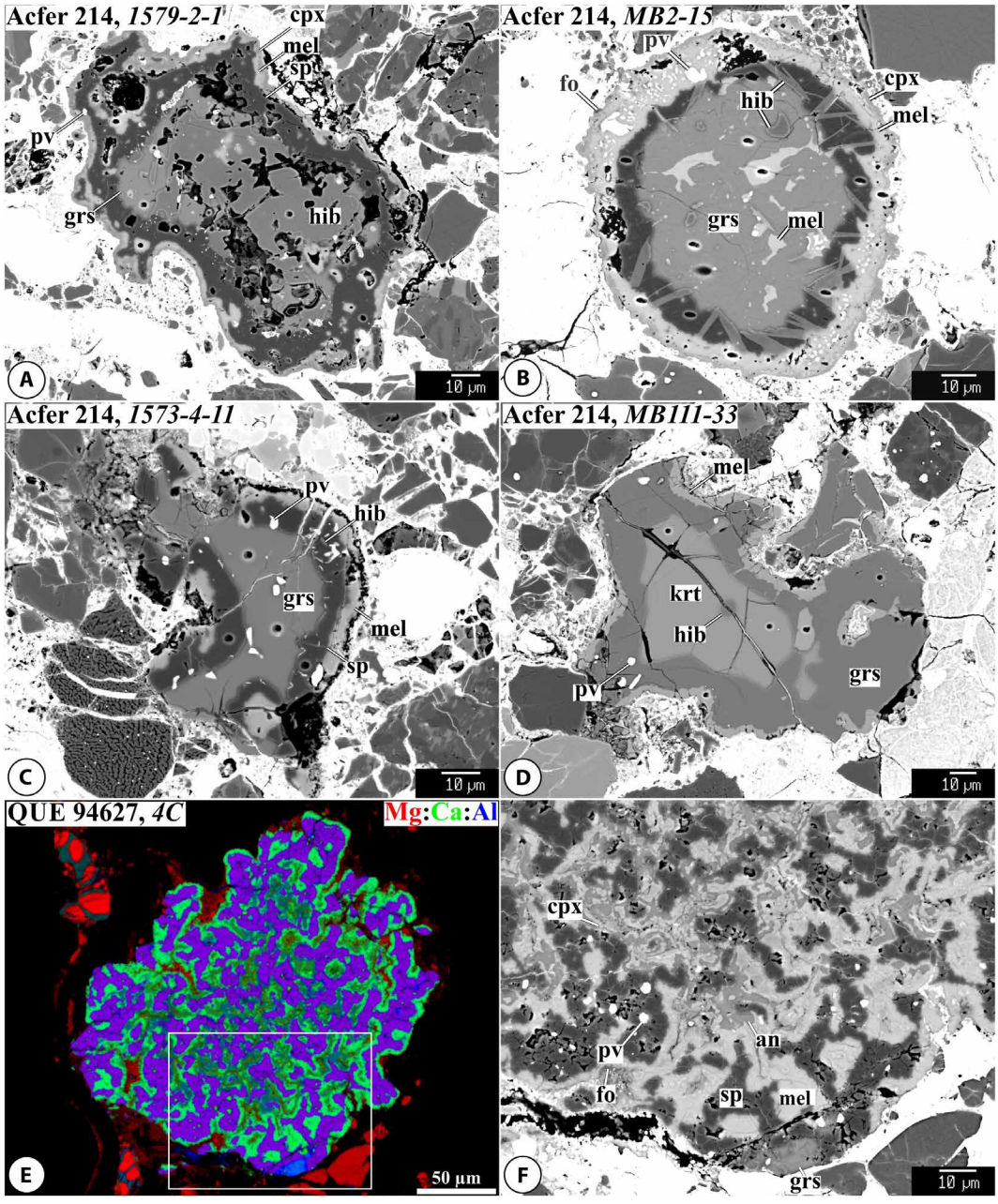

Fig. 1. Mineralogy and petrography of grossite-bearing CAIs in the metal-rich CH and CB carbonaceous chondrites. (**A** to **D** and **F**) Backscattered electron images and (**E**) combined x-ray elemental map in Mg (red), Ca (green), and Al (blue) of the grossite-bearing CAIs (A) *1579-2-1*, (B) *MB2-15*, (C) *1573-4-11*, (D) *MB111-33*, and (E and F) *4C* from Acfer 214 (CH) and QUE 94627 (CB). The region outlined in (E) is shown in (F). The Acfer 214 CAIs are surrounded by single- or multilayered Wark-Lovering rims, which are considered to have resulted from melting, evaporation, and condensation processes in the CAI-forming region. CAI *4C* is a fine-grained inclusion that probably represents an aggregate of nebular condensates. Cpx, Al-diopside; fo, forsterite; grs, grossite; hib, hibonite; krt, krotite; mel, melilite; pv, perovskite; sp., spinel.

FUN (fractionation and unidentified nuclear effects) CAIs, and some CAIs rich in corundum (Al_2O_3), hibonite ($CaAl_{12}O_{19}$), or grossite ($CaAl_4O_7$)] have much lower $(^{26}Al/^{27}Al)_0$ than the canonical value, $<5 \times 10^{-6}$ [e.g., (*25*–*28*, *33*, *34*)], hereafter referred to as ^{26}Al-poor CAIs. The ^{26}Al-poor CAIs are thought to have formed before injection and homogenization of ^{26}Al in the protoplanetary disk at the canonical level (*25*–*28*, *33*, *34*), i.e., before t_0. Because ^{26}Al appears to have been heterogeneously distributed in the CAI-forming region, the ^{26}Al-^{26}Mg relative chronology cannot be used for defining the age difference between the ^{26}Al-poor and ^{26}Al-rich inclusions and the duration of a CAI-forming epoch (*27*). Astrophysical modeling of a collapse of a protosolar molecular cloud externally polluted by stellar ^{26}Al suggests that ^{26}Al-poor CAIs may have formed within the first 10,000 to 20,000 years of the disk evolution, whereas the entire duration of CAI-forming epoch could have lasted ~200,000 to 300,000 years, when the Sun was a class 0-I star (*35*).

Grossite is one of the first minerals predicted to condense from a gas of solar composition (*36*). Although grossite-bearing CAIs are

quite rare in most chondrite groups, they are rather common in CH carbonaceous chondrites (*37*–*40*). The CH chondrites avoided thermal metamorphism and aqueous alteration on their parent body and therefore must have preserved nebular records largely unchanged (*39*). Most grossite-bearing CH CAIs are characterized by low $(^{26}Al/^{27}Al)_0$, typically $<10^{-6}$, consistent with being very ancient refractory inclusions (*24*, *37*, *38*, *40*). To understand the location of CO self-shielding (molecular cloud versus outer disk), we measured oxygen isotopic compositions (see Materials and Methods) of about 30 randomly selected grossite-bearing refractory inclusions in the paired CH chondrites Acfer 182 and Acfer 214. In the following discussion, we combine these data with the previously reported oxygen-isotope compositions of several grossite-bearing CAIs and AOAs in the genetically related CH3.0 and CB3.0 metal-rich carbonaceous chondrites (*24*, *40*–*43*).

RESULTS

Most grossite-bearing CAIs measured for oxygen-isotope compositions are isolated inclusions composed of grossite, ±hibonite, ±krotite, perovskite, spinel, and ±gehlenitic melilite, and surrounded by single (melilite)–layered or multilayered Wark-Lovering rims of spinel, ±hibonite, ±perovskite, melilite, and Al-diopside (Fig. 1, A to D). A grossite-bearing CAI *4C* from the CB chondrite QUE 94627 is a fine-grained inclusion composed of concentrically zoned objects made of (from core to edge) ±grossite, spinel, melilite, ±anorthite, diopside, and forsterite with inclusions of Fe,Ni-metal (Fig. 1, E and F). Two grossite-bearing CAIs, *1573-3-13* and *1-3*, are constituents of AOAs (fig. S1, A to D) (*40*). Several grossite-bearing CAIs occur as relict inclusions surrounded by a monomineralic spinel layer within the CH porphyritic chondrules (fig. S1, E and F) (*43*). All CAIs studied are mineralogically pristine and show no evidence for parent body metasomatic alteration or thermal metamorphism.

Oxygen isotopic compositions of the grossite-bearing CAIs studied are listed in table S1 and shown in Fig. 2. Only 2 of 41 (~5%) grossite-bearing inclusions measured from the CH, CH/CB, and CB chondrites, *1573-4-11* (Fig. 1C) and *1573-3-19* (fig. S1G), have heterogeneous oxygen isotopic compositions. In the CAI *1573-4-11*, the spinel layer of the Wark-Lovering rim is ^{16}O-enriched relative to grossite core ($\Delta^{17}O \sim -24$ and −17‰, respectively; because of a small size, the outermost melilite layer has not been analyzed). In the CAI *1573-3-19*, Al,Ti-diopside near the CAI edge is ^{16}O-enriched relative to grossite core and the spinel layer of the Wark-Lovering rim [$\Delta^{17}O \sim -27$‰ versus ~−22‰, respectively; the anorthite and diopside layers are too thin for our secondary ion mass spectrometry (SIMS) measurements]. The remaining inclusions are isotopically uniform within the analytical uncertainties of our SIMS measurements ($2\sigma \sim \pm 2$‰). There is, however, a large range of $\Delta^{17}O$ between individual inclusions, from ~−40 to ~−10‰. The fine-grained grossite-bearing CAI *4C* (Fig. 1, E and F) is uniformly ^{16}O-depleted ($\Delta^{17}O \sim -10$‰). The relict grossite-rich CAIs *MB4-1-5* (fig. S1E) and *MB1-1-1* (fig. S1F) inside porphyritic chondrules are isotopically uniform ($\Delta^{17}O \sim -33$ and ~−5‰, respectively) and compositionally distinct from the host chondrule phenocrysts ($\Delta^{17}O \sim +1$ and ~−2‰, respectively).

Only 3 of 59 (~5%) grossite-bearing CH CAIs measured for Al-Mg isotope systematics (*24*, *37*, *38*, *40*, *43*), including CAIs in AOAs and relict CAIs in chondrules, show high excesses of radiogenic ^{26}Mg corresponding to approximately the canonical $(^{26}Al/^{27}Al)_0$ of ~(4 to 5) × 10^{-5}. The remaining CAIs show either no evidence for resolvable excess of radiogenic ^{26}Mg or they show excesses corresponding to $(^{26}Al/^{27}Al)_0 < 5 \times 10^{-6}$ (Fig. 3A).

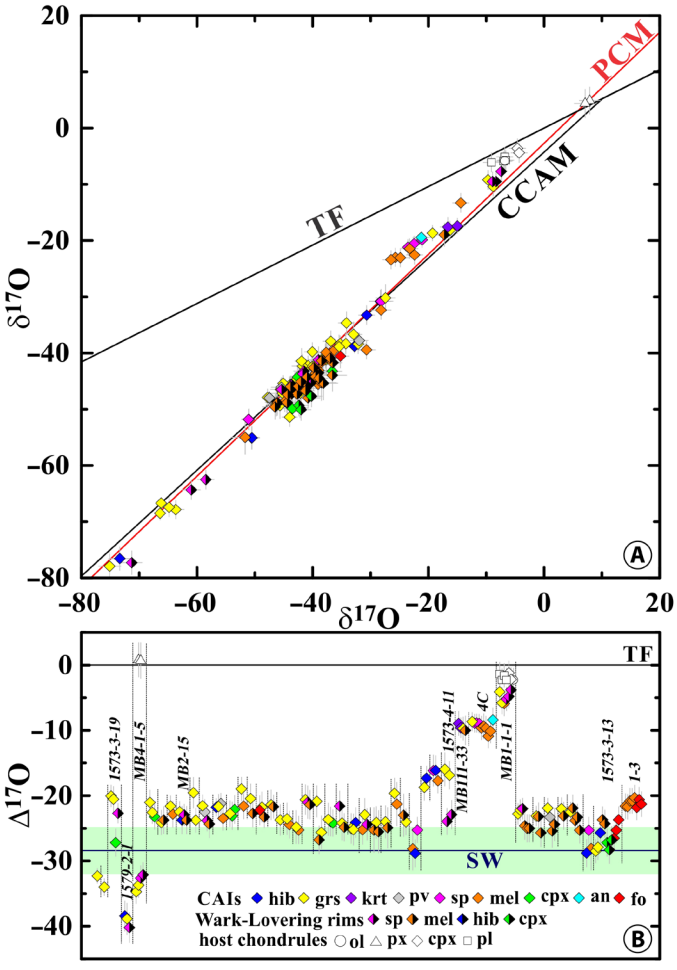

Fig. 2. Oxygen isotopic compositions of grossite-bearing CAIs in the metal-rich CH and CB carbonaceous chondrites. (**A**) $\delta^{17}O$ versus $\delta^{18}O$ and (**B**) $\Delta^{17}O$ of grossite-bearing CAIs, their Wark-Lovering rims, and CAI-bearing chondrules in CH, CH/CB, and CB metal-rich carbonaceous chondrites. In (B), individual CAIs are separated by dashed lines; numbered CAIs are shown in Fig. 1 and fig. S1. The vast majority of the CAIs studied have uniform $\Delta^{17}O$. There is, however, a large range of $\Delta^{17}O$ among individual inclusions. CAI minerals are shown by color symbols: an, anorthite; cpx, Al-diopside; fo, forsterite; grs, grossite; hib, hibonite; krt, krotite; mel, melilite; pv, perovskite; sp., spinel. Chondrule minerals are shown by black-and-white symbols: cpx, high-Ca pyroxene; ol, olivine; pl. plagioclase; px, low-Ca pyroxene. CCAM, carbonaceous chondrite anhydrous mineral line (*53*); PCM, primitive chondrule mineral line (*54*); SW, Genesis solar wind (*1*); TF, terrestrial fractionation line.

DISCUSSION

The observed range of $\Delta^{17}O$, from ~−40 to ~−10‰, among the isotopically uniform grossite-bearing CH and CB CAIs surrounded by Wark-Lovering rims and the uniformly ^{16}O-depleted grossite-bearing, fine-grained spinel-rich inclusion in QUE 94627 provide a strong evidence for the existence of gaseous reservoirs with different oxygen isotopic composition in the CH and CB CAI-forming region (*6*). (i) The fine-grained spinel-rich CAIs formed by aggregation of nebular

condensates and avoided subsequent melting (*22*). (ii) Wark-Lovering rim layers are thought to have formed by melt evaporation and condensation in the CAI-forming region (*42*). Therefore, the presence of Wark-Lovering rims around the isotopically uniform grossite-bearing CAIs studied, both having similar $\Delta^{17}O$, precludes late-stage reprocessing of these CAIs and oxygen-isotope exchange outside the CAI-forming region. For example, melting of CAIs in an ^{16}O-poor nebular gas during chondrule formation resulted in partial or complete destruction of Wark-Lovering rims and extensive oxygen-isotope exchange in the melted CAI minerals; the unmelted, relict CAI minerals, however, preserved their initial oxygen isotopic compositions (*43*). Relict grossite-bearing CAIs *MB4-1-5* and *MB1-1-1* inside porphyritic chondrules are surrounded by a monomineralic layer of spinel, which probably represents the innermost Wark-Lovering rim layer that survived melting during chondrule formation; the missing melilite and diopside layers were probably dissolved in the host chondrule melts (*42*, *43*). The rim spinels are compositionally very similar to grossite and melilite of the relict CAI cores. The host chondrule phenocrysts are ^{16}O-depleted compared to the relict CAIs (Fig. 3A). We infer that *MB4-1-5* and *MB1-1-1* largely preserved their original $\Delta^{17}O$, ~−33 and ~−5‰, respectively. Therefore, the entire range of $\Delta^{17}O$ of nebular gas recorded by the grossite-bearing CH and CB CAIs is from ~−40 to ~−5‰.

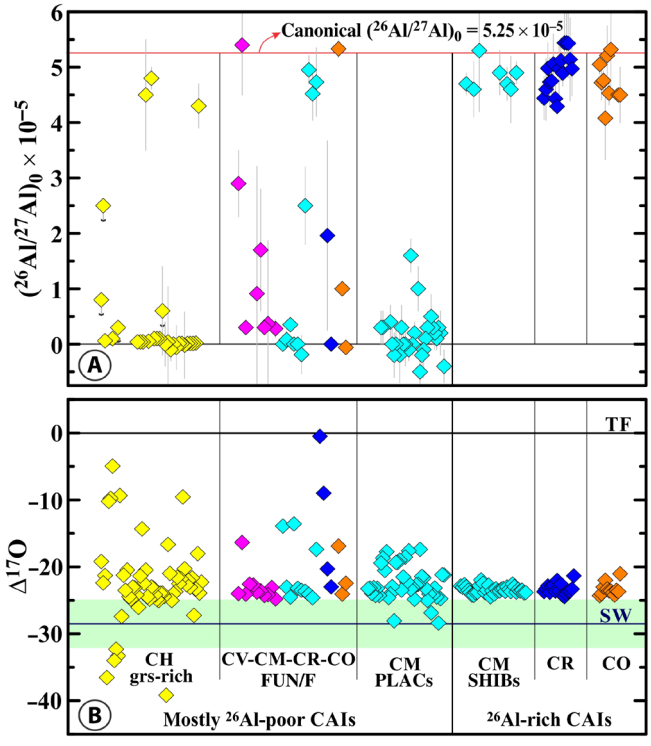

Fig. 3. The inferred initial $^{26}Al/^{27}Al$ ratios and $\Delta^{17}O$ values for CAIs from the CV3, CR2, CM2, CH3.0, and CO3.0-3.1 + Acfer 094 (C3.0 ungrouped) carbonaceous chondrites. (**A**) The initial $^{26}Al/^{27}Al$ [$(^{26}Al/^{27}Al)_0$] ratios inferred from the internal and model ^{26}Al-^{26}Mg isochrons in CAIs from the CV3, CR2, CM2, CH3.0, and CO3.0-3.1 + Acfer 094 (C3.0 ungrouped) carbonaceous chondrites. The CM SHIBs and CAIs in CR, CO, and CO-like chondrites have approximately the canonical $(^{26}Al/^{27}Al)_0$ of $(5.25 \pm 0.02) \times 10^{-5}$. The CM PLACs, most FUN/F (fractionation ± unidentified nuclear isotope effects) CAIs from CV, CM, CR, and CO chondrites, and ~95% of the grossite-bearing CH CAIs have much lower $(^{26}Al/^{27}Al)_0$ than the canonical value, $<5 \times 10^{-6}$. (**B**) Average $\Delta^{17}O$ of the isotopically uniform CAIs in CM2, CR2, CO3.0, CH3.0, and Acfer 094, and FUN/F CAIs from CV3, CO3, CM2, and CR2 chondrites. FUN CAIs from metamorphosed CV chondrites experienced postcrystallization oxygen-isotope exchange and are isotopically heterogeneous (*49*). To calculate the average $\Delta^{17}O$ of the CV FUN CAIs, only minerals that avoided postcrystallization oxygen-isotope exchange were used; these include spinel, hibonite, forsterite, and most Al,Ti-diopside grains. The predominantly ^{26}Al-poor CAIs show a much larger range of $\Delta^{17}O$ than the ^{26}Al-rich CAIs. Note that not all CAIs measured for oxygen isotopes were analyzed for Al-Mg isotope systematics. Data from (*8*–*10*, *24*, *26*, *28*, *32*, *34*, *37*, *38*, *49*, *40*–*43*) and this study. grs, grossite; ; SW, Genesis solar wind (*1*); TF, terrestrial fractionation line.

Two grossite-bearing CAIs showing variations in $\Delta^{17}O$, *1573-4-11* and *1573-3-19*, appear to have recorded fluctuations of oxygen isotopic composition of nebular gas during their formation. In the CAI *1573-4-11*, the spinel layer of the Wark-Lovering rim is ^{16}O-enriched relative to grossite core. We infer that oxygen-isotope composition of the nebular gas changed from ^{16}O-depleted to ^{16}O-rich during crystallization of spinel. Bodénan *et al.* (*44*) have reported fluctuation of oxygen-isotope composition of nebular gas in the opposite direction during condensation of a diopside rim ($\Delta^{17}O$ ~ −25‰) around corundum-hibonite-spinel CAI ($\Delta^{17}O$ ~ −33‰) from the ALH 77307 (CO3.0) chondrite. Cyclical fluctuations of O-isotope composition of nebular gas during growth of a spinel-rich layered CAI from the MIL 090019 (CO3) chondrite have been inferred by Simon *et al.* (*45*). In the CAI *1573-3-19*, Al,Ti-diopside near the CAI edge is ^{16}O-enriched relative to the grossite core and the spinel layer of a discontinuous spinel-anorthite-diopside Wark-Lovering rim. In this case, we cannot exclude change in oxygen-isotope composition of the nebular gas after formation of the Wark-Lovering rim, e.g., during partial melting.

There are three major oxygen-bearing species in the protosolar molecular cloud: CO, H_2O, and silicates. The initial oxygen isotopic compositions of these species in the early Solar System are not known. FUV (far ultraviolet) CO self-shielding in the protosolar molecular cloud (*16*) or in the outer protoplanetary disk (*17*) is expected to produce ^{16}O-rich CO and ^{16}O-poor H_2O. The primordial silicates in molecular clouds are largely amorphous (*46*), and their oxygen isotopic compositions are not directly affected by the CO self-shielding at low temperatures (<50 K) expected for these environments, because oxygen-isotope exchange between amorphous silicates and water requires much higher temperatures, >500 K (*47*). Assuming that primordial silicates had a solar $\Delta^{17}O$ of −28.8‰, whereas CO and H_2O were ^{16}O-rich ($\Delta^{17}O$ = −116‰) and ^{16}O-depleted ($\Delta^{17}O$ = +24‰), respectively, Alexander *et al.* (*48*) calculated that evaporation of disk regions enriched in primordial silicates and water-dominated ice relative to CO gas [dust/gas ratio ~ (1 to 5) × solar] could produce nebular gas with $\Delta^{17}O$ ranging from −28.8 to ~−5‰; evaporation of dust-depleted regions (~0.6 × solar) could produce nebular gas enriched in ^{16}O relative to the Sun, with a $\Delta^{17}O$ of ~−40‰. Therefore, this process could explain the entire range of $\Delta^{17}O$ values recorded by the grossite-bearing CH studied. We note that two other types of ^{26}Al-poor refractory inclusions, PLACs (*28*) and FUN CAIs (*49*), also show a larger range of $\Delta^{17}O$ compared to the ^{26}Al-rich CAIs in CR (*8*), CM (*9*), and CO (*10*, *11*) chondrites (Fig. 3, A and B).

Quantitative modeling of the CO self-shielding in the parent molecular cloud core illustrates how the self-shielding process may have operated. Model results from Lee *et al.* (*50*) for CO self-shielding in a collapsing cloud core predict massive ^{16}O enrichments and depletions in the CO and H_2O ice reservoirs, respectively. The protostellar core

collapse is modeled as a sequence of Bonnor-Ebert spheres that undergo densification with each step in the sequence, with seven steps total. At time $t = 0$ in the collapse model, growth of the protosun commences. After 4.6×10^5 years, the protosun has reached a mass of 1 M_{Sun}. Figures 4 and 5 show volume fractions and delta values for several important chemical species in the collapse model, including gaseous CO, CO_{ice}, and H_2O_{ice} at the inner edge of the model (125 AU) and for a FUV radiation field that is 100× the local interstellar field ($G_0 = 100$). Most of the collapsing material goes to the formation of the protosun, and all self-shielding–derived isotope signatures are erased in this material owing to high-temperature exchange. Higher angular momentum material falls further out onto the growing disk (*35*). If the temperature of the infall material accreted onto the disk is sufficiently low that trapping of ^{16}O-poor (^{17,18}O-rich) H_2O ice on dust particles occurs, subsequent gravitational settling of icy grains creates an ^{16}O-poor zone (H_2O ice) near the developing midplane and an ^{16}O-rich zone near the surface (CO). Ice/gas separation is an essential component of the CO self-shielding theory for the distribution of oxygen isotopes in inner Solar System materials (*16*, *17*) and provides a natural explanation for the Δ^{17}O values of the grossite-rich CAIs reported here. The isotopic result of material fractionation of H_2O ice and CO gas for the inner edge of the collapse model is shown in Fig. 6. For this model run, which assumes a FUV radiation field that is 100× the local interstellar medium field, approximately 10% of H_2O ice must be sequestered on grains during inward migration of nebular material. A coupled collapse-disk model with all oxygen isotopologues and chemical kinetics is needed to fully quantify this scenario. Ideally, a three-dimensional simulation is needed with an anisotropic radiation field and possible dynamical effects to account for possible intracloud variations in self-shielding isotope signatures.

CO self-shielding also likely occurred early in the outer solar nebula. Because the formation of ^{26}Al-poor CAIs may have occurred within the first 20,000 to 30,000 years of the protoplanetary disk evolution (*35*), nebular self-shielding would require rapid transfer of CO to the inner disk (~10^4 years for a turbulent viscosity parameter $\alpha \sim 0.1$; fig. S2) to account for the very low Δ^{17}O values of CAIs reported here. In this scenario, a zone of ^{16}O-enriched CO is formed between the UV disk surface and the deeper x-ray surface, with FUV photons creating the $^{12}C^{16}O$ enrichment and x-rays generating enough ionization to form the high-α region (fig. S3A). H_2O derived from CO self-shielding must first be trapped on grains and fall out of the high-α UV active zone. Calculations show that this may be possible on a time scale of ~10^4 years, but this assumes a disk structure similar to the post-infall accretion disk, a structure unlikely to be valid shortly after the start of infall. In addition, the observation that the range of Δ^{17}O of CAIs with the canonical $(^{26}Al/^{27}Al)_0$ is very limited (Fig. 3) suggests that CO and H_2O were isotopically homogenized with time until the arrival of ^{16}O-poor H_2O brought in by centimeter-scale ice-rich objects. We hypothesize that this contradicts continuous generations of oxygen isotopic effects by CO self-shielding in the outer disk but is consistent with inheritance of isotopic effects in CO and H_2O from the molecular cloud. A time-evolving coupled collapse-disk model with vertical and radial transport, chemical kinetics, and all oxygen isotopologues is needed to fully evaluate this scenario.

We conclude that the origin of the oxygen isotope variations seen in Solar System materials most likely derives from self-shielding of CO in the parent molecular cloud from which the Solar System formed. Photodissociation and material fractionation (i.e., H_2O ice sequestration on grains) were primary determinants of the distribution

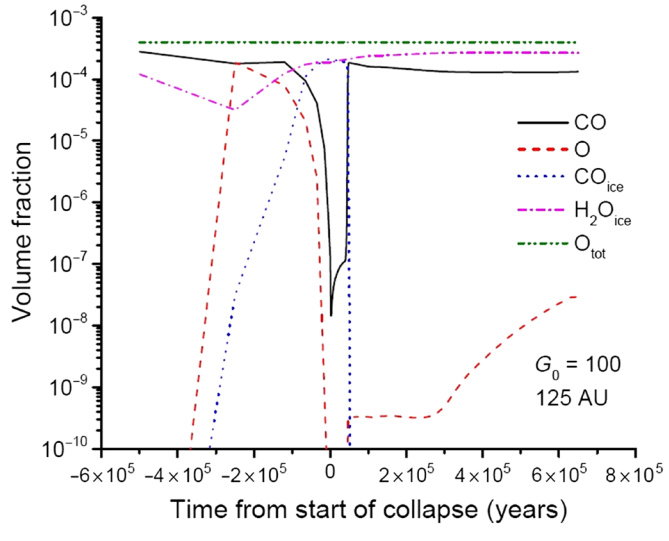

Fig. 4. Volume fractions of key O-bearing species in the protostellar collapse model of Lee *et al.* at the inner boundary of the model (125 AU). Volume fractions of key O-bearing species in the Lee *et al.* (*50*) protostellar collapse model at the inner boundary of the model (125 AU). The radiation field is 100× the local interstellar medium FUV radiation field ($G_0 = 100$). Collapse is defined to start at $t = 0$. The first CAIs are believed to have formed ~10^4 years after the start of the collapse. The photochemical loss of CO releases oxygen atoms that are converted to H_2O.

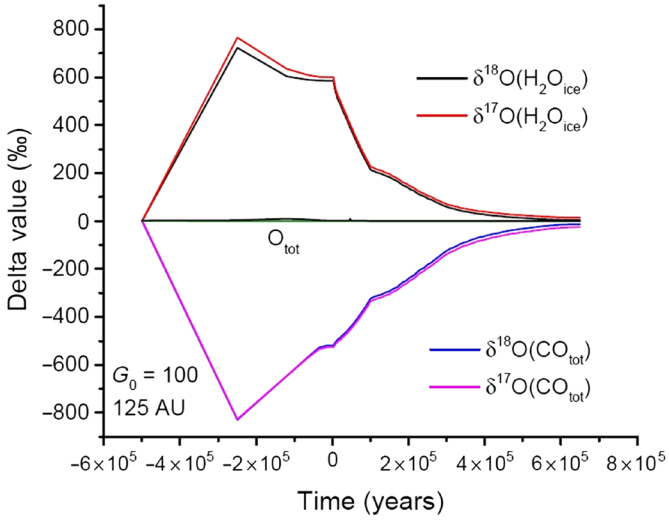

Fig. 5. Time evolution of delta values (δ^{17}O and δ^{18}O) for CO and H_2O at the inner boundary of the collapse model of Lee *et al.* Time evolution of delta values (δ^{17}O and δ^{18}O) for CO and H_2O at the inner boundary of the collapse model of Lee *et al.* (*50*). Delta values are computed relative to initial (assumed) molecular cloud ratios; delta values relative to SMOW (Standard Mean Ocean Water) would be approximately 60‰ lighter. $CO_{tot} = CO + CO_{ice}$ and $O_{tot} = CO_{tot} + H_2O_{ice}$ + atomic O. At time $t = 0$, the protosun begins to accumulate mass. At the end of the model run, the protosun is 1 solar mass. Photodissociation of CO is accompanied by a massive isotope enrichment in ^{17}O and ^{18}O in the newly formed H_2O due to self-shielding by $^{12}C^{16}O$. CO isotope fractionation during photodissociation is computed using shielding functions.

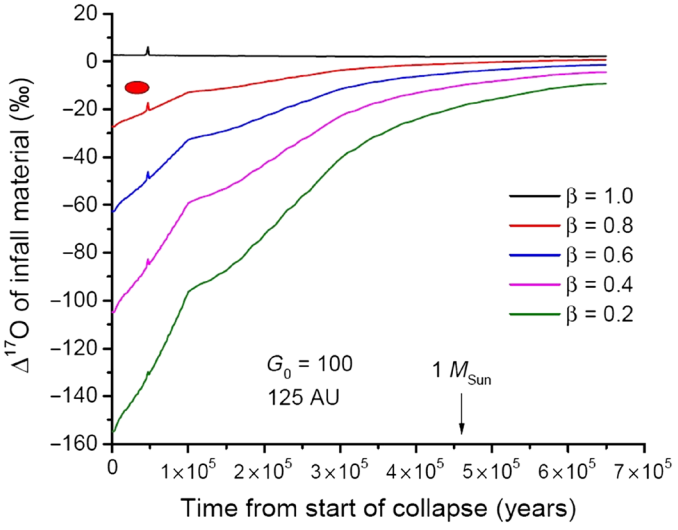

Fig. 6. Time evolution of Δ^{17}O of fractionated nebular material ($CO + H_2O + O$) at the inner edge of the collapse model. Time evolution of Δ^{17}O of fractionated nebular material ($CO + H_2O + O$) at the inner edge of the collapse model. Dust/gas fractionation between $CO + O$ and H_2O is accounted for by the factor β, which is the fraction of H_2O remaining in nebular material transported to the inner disk. This would be the Δ^{17}O value of the CAI-forming region. The Δ^{17}O values are relative to the bulk initial cloud, which we assume to be identical to the modern bulk Sun. Δ^{17}O values of ~−10‰ are required to explain the lowest Δ^{17}O value of ^{26}Al-poor CH CAI data presented here, indicated by the red ellipse at a time ~20,000 to 30,000 years after the start of collapse. In the collapse model, the protosun is fully formed by 4.6×10^5 years. Results from the model described in Lee *et al.* (*50*).

of oxygen isotopes in planetary materials formed in the solar nebula. Future modeling of isotope exchange reactions during accretion of cloud core material will very likely yield a strong constraint on the size of the stellar nursery that gave birth to our Solar System.

MATERIALS AND METHODS

To search for grossite-bearing CAIs, multiple polished sections of Acfer 182 and Acfer 214 were mapped in Mg, Ca, Al, and Ti Kα rays using a 10-μm electron beam, a 15-kV accelerating voltage, a 50-nA beam current, an acquisition time of 10 ms per pixel, and a resolution of 10 μm per pixel with wavelength-dispersive spectrometer detectors with the University of Hawai'i's field-emission electron microprobe JEOL JXA-8500F. Elemental maps in Mg, Ca, and Al Kα were combined using an RGB color scheme (Mg, red; Ca, green; and Al, blue). In these maps, the grossite-bearing CAIs have a dark-blue color. The identified inclusions were studied in backscattered electrons and analyzed for chemical compositions using the UH JEOL JXA-8500F. Quantitative wavelength-dispersive analyses were obtained at 15 kV with counting times of 30 s for peak and for background measurements for each analysis. Natural minerals were used as standards. Electron probe data were reduced via the modified ZAF (Z is the atomic number correction, A is the absorption correction, F is the fluorescence correction) correction procedure PAP (*51*).

Oxygen isotopic compositions were analyzed in situ with the UH Cameca ims-1280 ion microprobe using the previously described method (*52*). Briefly, a primary Cs^+ ion beam focused to ~1 to 2 μm with ~25 pA was used. Three oxygen isotopes were measured simultaneously: $^{16}O^-$ was measured on a Faraday cup, and $^{17}O^-$ and $^{18}O^-$ were measured on electron multipliers. Instrumental fractionation was corrected using terrestrial standards, including San Carlos olivine (for melilite, olivine, and low-Ca pyroxene), augite (for Al-diopside and high-Ca pyroxene), spinel (for hibonite, grossite, krotite, spinel, and perovskite), and Miyake-jima anorthite (for plagioclase).

SUPPLEMENTARY MATERIALS

Supplementary material for this article is available at http://advances.sciencemag.org/cgi/content/full/6/42/eaay2724/DC1

REFERENCES AND NOTES

1. K. D. McKeegan, A. P. A. Kallio, V. S. Heber, G. Jarzebinski, P. H. Mao, C. D. Coath, T. Kunihiro, R. C. Wiens, J. E. Nordholt, R. W. Moses Jr., D. B. Reisenfeld, A. J. G. Jurewicz, D. S. Burnett, The oxygen isotopic composition of the Sun inferred from captured solar wind. *Science* **332**, 1528–1532 (2011).
2. R. N. Clayton, T. K. Mayeda, J. N. Goswami, E. J. Olsen, Oxygen isotope studies of ordinary chondrites. *Geochim. Cosmochim. Acta* **55**, 2317–2337 (1991).
3. R. N. Clayton, T. K. Mayeda, Oxygen isotope studies of carbonaceous chondrites. *Geochim. Cosmochim. Acta* **63**, 2089–2104 (1999).
4. A. N. Krot, K. Keil, C. Goodrich, E. R. D. Scott, M. K. Weisberg, Classification of meteorites, in *Treatise on Geochemistry, Vol. 1: Meteorites, Comets, and Planets*, A. M. Davis, Ed. (Elsevier, Oxford, 2014), pp. 1–63.
5. T. J. Tenner, T. Ushikubo, D. Nakashima, D. L. Schrader, M. K. Weisberg, M. Kimura, N. Kita, Oxygen isotope characteristics of chondrules from recent studies by secondary ion mass spectrometry, in *Chondrules: Records of the Protoplanetary Disk Processes*, S. S. Russel, H. C. Connolly Jr., A. N. Krot, Eds. (Cambridge Univ. Press, 2018), pp. 196–247.
6. H. Yurimoto, A. N. Krot, B.-G. Choi, J. Aléon, T. Kunihiro, A. J. Brearley, Oxygen isotopes of chondritic components, in *Oxygen in the Solar System*, G. J. MacPherson, Ed. (2008), *Rev. Mineral. Geochem.*, vol. 68, pp. 141–187.
7. S. Kobayashi, H. Imai, H. Yurimoto, New extreme ^{16}O-rich reservoir in the early solar system. *Geochem. J.* **37**, 663–669 (2003).
8. K. Makide, K. Nagashima, A. N. Krot, G. R. Huss, I. D. Hutcheon, A. Bischoff, Oxygen- and magnesium-isotope compositions of calcium-aluminum-rich inclusions from CR2 carbonaceous chondrites. *Geochim. Cosmochim. Acta* **73**, 5018–5051 (2009).
9. L. Kööp, D. Nakashima, P. R. Heck, N. T. Kita, T. J. Tenner, A. N. Krot, K. Nagashima, C. Park, A. M. Davis, New constraints for the relationship between ^{26}Al and oxygen, calcium, and titanium isotopic variation in the early Solar System from a multi-element isotopic study of Spinel-Hibonite inclusions. *Geochim. Cosmochim. Acta* **184**, 151–172 (2016).
10. T. Ushikubo, T. J. Tenner, H. Hiyagon, N. T. Kita, A long duration of the ^{16}O-rich reservoir in the solar nebula, as recorded in fine-grained refractory inclusions from the least metamorphosed carbonaceous chondrites. *Geochem. Cosmochim. Acta* **201**, 103–122 (2017).
11. S. B. Simon, A. N. Krot, K. Nagashima, Oxygen and Al-Mg isotopic compositions of grossite-bearing refractory inclusions from CO3 chondrites. *Meteorit. Planet. Sci.* **54**, 1362–1378 (2019).
12. J. T. Wasson, H. Yurimoto, S. S. Russell, ^{16}O-rich melilite in CO3.0 chondrites: Possible formation of common, ^{16}O-poor melilite by aqueous alteration. *Geochim. Cosmochim. Acta Theriol.* **65**, 4539–4549 (2001).
13. A. N. Krot, K. Nagashima, K. Fintor, E. Pál-Molnár, Evidence for oxygen-isotope exchange in refractory inclusions from Kaba (CV3.1) carbonaceous chondrite during fluid-rock interaction on the CV parent asteroid. *Geochim. Cosmochim. Acta Theriol.* **246**, 419–435 (2019).
14. M. H. Thiemens, J. E. Heidenreich III, The mass independent fractionation of oxygen: A novel isotopic effect and its possible cosmochemical implications. *Science* **219**, 1073–1075 (1983).
15. R. N. Clayton, Solar system: Self-shielding in the solar nebula. *Nature* **415**, 860–861 (2002).
16. H. Yurimoto, K. Kuramoto, Molecular cloud origin for the oxygen-isotope heterogeneity in the solar system. *Science* **305**, 1763–1766 (2004).
17. J. R. Lyons, E. D. Young, CO self-shielding as the origin of oxygen isotope anomalies in the early solar nebula. *Nature* **435**, 317–320 (2005).
18. J. R. Lyons, E. D. Young, Towards an evaluation of self-shielding at the X-point as the origin of the oxygen isotope anomaly in CAIs. *Lunar Planet. Sci.* **34**, 1981 (2003).
19. N. Sakamoto, Y. Seto, S. Itoh, K. Kuramoto, K. Fujino, K. Nagashima, A. N. Krot, H. Yurimoto, Remnants of the early solar system water enriched in heavy oxygen isotopes. *Science* **317**, 231–233 (2007).

20. J. N. Connelly, M. Bizzarro, A. N. Krot, Å. Nordlund, D. Wielandt, M. A. Ivanova, The absolute chronology and thermal processing of solids in the solar protoplanetary disk. *Science* **338**, 651–655 (2012).
21. K. D. McKeegan, M. Chaussidon, F. Robert, Incorporation of short-lived ^{10}Be in a calcium–aluminum-rich inclusion from the Allende meteorite. *Science* **289**, 1334–1337 (2000).
22. G. J. MacPherson, Calcium-aluminum-rich inclusions in chondritic meteorites, in *Meteorites, Comets and Planets, Vol. 1, Treatise on Geochemistry*, A. M. Davis, Ed. (Elsevier, Oxford, 2014), pp. 139–179.
23. S. B. Simon, A. M. Davis, L. Grossman, K. D. McKeegan, A hibonite-corundum inclusion from Murchison: A first-generation condensate from the solar nebula. *Meteorit. Planet. Sci.* **37**, 548–548 (2002).
24. A. N. Krot, K. Nagashima, M. Bizzarro, G. R. Huss, A. M. Davis, B. S. Meyer, A. A. Ulyanov, Multiple generations of refractory inclusions in the metal-rich carbonaceous chondrites Acfer 182/214 and Isheyevo. *Astrophys. J.* **672**, 713–721 (2008).
25. S. Sahijpal, G. N. Goswami, Refractory phases in primitive meteorites devoid of ^{26}Al and ^{41}Ca: Representative samples of first solar system solids? *Astrophys. J.* **509**, L137–L140 (1998).
26. M.-C. Liu, K. D. McKeegan, J. N. Goswami, K. K. Marhas, S. Sahijpal, T. R. Ireland, A. M. Davis, Isotopic records in CM hibonites: Implications for timescales of mixing of isotope reservoirs in the solar nebula. *Geochim. Cosmochim. Acta* **73**, 5051–5079 (2009).
27. A. N. Krot, K. Makide, K. Nagashima, G. R. Huss, R. C. Ogliore, F. J. Ciesla, L. Yang, E. Hellebrand, E. Gaidos, Heterogeneous distribution of ^{26}Al at the birth of the solar system: Evidence from refractory grains and inclusions. *Meteorit. Planet. Sci.* **47**, 1948–1979 (2012).
28. L. Kööp, A. M. Davis, D. Nakashima, C. Park, A. N. Krot, K. Nagashima, T. J. Tenner, P. R. Heck, N. T. Kita, A link between oxygen, calcium and titanium isotopes in ^{26}Al-depleted hibonite-rich CAIs from Murchison and implications for the heterogeneity of dust reservoirs in the solar nebula. *Geochim. Cosmochim. Acta* **189**, 70–95 (2016).
29. E. Gaidos, A. N. Krot, J. P. Williams, S. N. Raymond, ^{26}Al and the formation of the solar system from a molecular cloud contaminated by Wolf-Rayet winds. *Astrophys. J.* **696**, 1854–1863 (2009).
30. V. V. Dwarkadas, N. Dauphas, B. Meyer, P. Boyajian, M. Bojazi, Triggered star formation at the periphery of the shell of a Wolf-Rayet bubble as the origin of the solar system. *Lunar Planet. Sci.* **851**, 147 (2017).
31. M. Gounelle, G. Meynet, Solar system genealogy revealed by extinct short-lived radionuclides in meteorites. *Astron. Astrophys.* **545**, A4 (2012).
32. K. Larsen, K. K. Larsen, A. Trinquier, C. Paton, M. Schiller, D. Wielandt, M. A. Ivanova, J. Connelly, Å. Nordlund, A. Krot, M. Bizzarro, Evidence for magnesium-isotope heterogeneity in the solar protoplanetary disk. *Astrophys. J.* **735**, L37–L40 (2011).
33. K. Makide, K. Nagashima, A. N. Krot, G. R. Huss, I. D. Hutcheon, E. Hellebrand, M. I. Petaev, Heterogeneous distribution of ^{26}Al at the birth of the solar system: Evidence from corundum-bearing refractory inclusions in carbonaceous chondrites. *Geochim. Cosmochim. Acta* **110**, 190–215 (2013).
34. C. Park, K. Nagashima, A. N. Krot, G. R. Huss, A. M. Davis, M. Bizzarro, Calcium-aluminum-rich inclusions with fractionation and unidentified nuclear effects (FUN CAIs): II. Heterogeneities of magnesium isotopes and ^{26}Al in the early solar system inferred from *in situ* high-precision magnesium-isotopic measurements. *Geochim. Cosmochim. Acta* **201**, 6–24 (2017).
35. F. C. Pignatale, F. Pignatale, S. Charnoz, M. Chaussidon, E. Jacquet, Making the planetary material diversity during the early assembling of the solar system. *Astrophys. J. Lett.* **867**, L23 (2018).
36. D. S. Ebel, Condensation of rocky material in astrophysical environments, in *Meteorites and The Early Solar System II*, D. Lauretta, H. McSween, Eds. (University of Arizona Press, 2006), p. 267.
37. M. Kimura, A. E. Goresy, H. Palme, E. Zinner, Ca-Al-rich inclusions in the unique chondrite ALH 85085–Petrology, chemistry, and isotopic compositions. *Geochim. Cosmochim. Acta* **57**, 2329–2359 (1993).
38. D. Weber, E. Zinner, A. Bischoff, Trace element abundances and magnesium, calcium, and titanium isotopic compositions of grossite-containing inclusions from the carbonaceous chondrite Acfer 182. *Geochim. Cosmochim. Acta* **59**, 803–823 (1995).
39. A. N. Krot, A. Meibom, M. K. Weisberg, K. Keil, The CR chondrite clan: Implications for early solar system processes. *Meteorit. Planet. Sci.* **37**, 1451–1490 (2002).
40. A. N. Krot, C. Park, K. Nagashima, Amoeboid olivine aggregates from CH carbonaceous chondrites. *Geochim. Cosmochim. Acta* **139**, 131–153 (2014).
41. M. Gounelle, A. N. Krot, K. Nagashima, A. Kearsley, Extreme ^{16}O-enrichment in calcium-aluminum-rich inclusions from the Isheyevo (ch/cb) chondrite. *Astrophys. J. Lett.* **698**, L18–L22 (2009).
42. A. N. Krot, K. Nagashima, E. M. M. van Kooten, M. Bizzarro, High-temperature rims around calcium-aluminum-rich inclusions from the CR, CB and CH carbonaceous chondrites. *Geochim. Cosmochim. Acta* **201**, 155–184 (2017).
43. A. N. Krot, K. Nagashima, E. M. M. van Kooten, M. Bizzarro, Calcium-aluminum-rich inclusions recycled during formation of porphyritic chondrules from CH carbonaceous chondrites. *Geochim. Cosmochim. Acta* **201**, 185–223 (2017).
44. J.-D. Bodénan, N. A. Starkey, S. S. Russell, I. P. Wright, I. A. Franchi, Large enrichments in ^{16}O and evidence for multiple reservoirs in the protosolar accretion disk in a corundum-bearing CAI. *Lunar Planet. Sci.* **45**, 2025 (2014).
45. J. I. Simon, D. K. Ross, A. N. Nguyen, S. B. Simon, S. Messenger, Molecular cloud origin for oxygen isotopic heterogeneity recorded by a primordial spinel-rich refractory inclusion. *Astrophys. J. Lett.* **884**, L29 (2019).
46. F. Kemper, W. J. Vriend, A. G. G. M. Tielens, The absence of crystalline silicates in the diffuse interstellar medium. *Astrophys. J.* **609**, 826–837 (2004).
47. D. Yamamoto, M. Kuroda, S. Tachibana, N. Sakamoto, H. Yurimoto, Oxygen isotopic exchange between amorphous silicate and water vapor and its implications for oxygen isotopic evolution in the early solar system. *Astrophys. J.* **865**, 98 (2018).
48. C. M. O.'D. Alexander, L. R. Nittler, J. Davidson, F. J. Ciesla, Measuring the level of interstellar inheritance in the solar protoplanetary disk. *Meteorit. Planet. Sci.* **52**, 1797–1821 (2017).
49. A. N. Krot, K. Nagashima, G. J. Wasserburg, G. R. Huss, D. Papanastassiou, A. M. Davis, I. D. Hutcheon, M. Bizzarro, Calcium-aluminum-rich inclusions with fractionation and unknown nuclear effects (FUN CAIs): I. Mineralogy, petrology, and oxygen-isotope compositions. *Geochim. Cosmochim. Acta* **145**, 206–247 (2014).
50. J.-E. Lee, E. A. Bergin, J. R. Lyons, Oxygen isotope anomalies of the Sun and the original environment of the solar system. *Meteorit. Planet. Sci.* **43**, 1351–1362 (2008).
51. J. L. Pouchou, F. Pichoir, A new model for quantitative x-ray microanalysis. Part I: Application to the analysis of homogeneous samples. *Rech. Aerosp.* **3**, 13–38 (1984).
52. K. Nagashima, A. N. Krot, G. R. Huss, Oxygen-isotope compositions of chondrule silicates and matrix grains in Kakangari K-grouplet chondrite: Implication to a chondrule-matrix genetic relationship. *Geochim. Cosmochim. Acta* **151**, 49–67 (2015).
53. R. N. Clayton, L. Grossman, T. K. Mayeda, A component of primitive nuclear composition in carbonaceous chondrites. *Science* **182**, 482–485 (1973).
54. T. Ushikubo, M. Kimura, N. T. Kita, J. W. Valley, Primordial oxygen isotope reservoirs of the solar nebula recorded in chondrules in Acfer 094 carbonaceous chondrite. *Geochim. Cosmochim. Acta* **90**, 242–264 (2012).
55. Y. Aikawa, E. Herbst, Molecular evolution in protoplanetary disks. Two-dimensional distributions and column densities of gaseous molecules. *Astron. Astrophys.* **351**, 233–246 (1999).
56. A. E. Glassgold, J. Najita, J. Igea, X-ray ionization of protoplanetary disks. *Astrophys. J.* **480**, 344–350 (1997).
57. E. I. Chiang, P. Goldreich, Spectral energy distributions of T Tauri stars with passive circumstellar disks. *Astrophys. J.* **490**, 368–376 (1997).
58. T. J. Millar, Astrochemistry. *Plasma Sources Sci. Technol.* **24**, 043001 (2015).
59. E. F. van Dishoeck, J. H. Black, The photodissociation and chemistry of interstellar CO. *Astrophys. J.* **334**, 771–802 (1988).
60. F. J. Ciesla, The distributions and ages of refractory objects in the solar nebula. *Icarus* **208**, 455–467 (2010).
61. T. Birnstiel, M. Fang, A. Johansen, Dust evolution and the formation of planetesimals. *Space Sci. Rev.* **205**, 41–75 (2016).
62. R. L. Smith, K. M. Pontoppidan, E. D. Young, M. R. Morris, E. F. van Dishoeck, High-precision $C^{17}O$, $C^{18}O$, and $C^{16}O$ measurements in young stellar objects: Analogues for CO self-shielding in the early solar system. *Astrophys. J.* **701**, 163–175 (2009).

Acknowledgments

Funding: This material is based on work supported by the NASA Emerging Worlds grants NNX17AE22G (A.N.K., PI) and 80NSSC18K0592 (J.R.L., PI). M.B. acknowledges funding from the Carlsberg Foundation (CF18_1105), the Danish National Research Foundation (DNRF97) and the European Research Council (ERC Advanced Grant Agreement 833275–DEEPTIME). J.-E.L. was supported by the Basic Science Research Program through the National Research Foundation of Korea (grant no. NRF-2018R1A2B6003423). **Author contributions:** A.N.K., K.N., and M.B. designed the study. A.N.K. and K.N. performed the mineralogic studies and isotopic measurements. J.R.L. and J.-E.L. performed calculations. A.N.K. and J.R.L. wrote the manuscript. **Competing interests:** The authors declare that they have no competing interests. **Data and materials availability:** All data needed to evaluate the conclusions in the paper are present in the paper and/or the Supplementary Materials. Additional data related to this paper may be requested from the authors.

Submitted 4 June 2019
Accepted 2 September 2020
Published 16 October 2020
10.1126/sciadv.aay2724

Citation: A. N. Krot, K. Nagashima, J. R. Lyons, J.-E. Lee, M. Bizzarro, Oxygen isotopic heterogeneity in the early Solar System inherited from the protosolar molecular cloud. *Sci. Adv.* **6**, eaay2724 (2020).